MATERIALS CHARACTERIZATION 59 (2008) 663–668

# Investigation on the intergranular corrosion resistance of the AISI 316L(N) stainless steel after long time creep testing at 600 °C

M. Terada[a,*], D.M. Escriba[b], I. Costa[a], E. Materna-Morris[c], A.F. Padilha[b,1]

[a]Instituto de Pesquisas Energéticas e Nucleares (IPEN), Centro de Ciência e Tecnologia de Materiais, Av. Lineu Prestes, 2242-Cidade Universitária-Butantã-CEP 05580-900-São Paulo-SP, Brazil
[b]Escola Politécnica da Universidade de São Paulo (EPUSP), Departamento de Engenharia Metalúrgica e de Materiais, Av. Prof. Mello Moraes, 2463-Cidade Universitária-Butantã-CEP 05580-900-São Paulo-SP, Brazil
[c]Forschungszentrum Karlsruhe (FZK), Institut für Materialforschung I, P. O. Box 3640, 76021 Karlsruhe, Germany

ARTICLE DATA

*Article history:*
Received 8 May 2007
Accepted 24 May 2007

*Keywords:*
Intergranular corrosion
AISI 316L(N) stainless steel
Creep test
Electrochemical techniques
Sigma phase precipitation

ABSTRACT

The effect of precipitation on the corrosion resistance of AISI 316L(N) stainless steel previously exposed to creep tests at 600 °C for periods of up to 10 years, has been studied. The corrosion resistance was investigated in 2 M $H_2SO_4$ + 0.5 M NaCl + 0.01 M KSCN solution at 30 °C by electrochemical methods. The results showed that the susceptibility to intergranular corrosion was highly affected by aging at 600 °C and creep testing time. The intergranular corrosion resistance decreased by more than twenty times when the creep testing time increased from 7500 h to 85,000 h. The tendency to passivation decreased and less protective films were formed on the creep tested samples. All tested samples also showed susceptibility to pitting. Grain boundary $M_{23}C_6$ carbides were not found after long-term exposure at 600 °C and the corrosion behavior of the creep tested samples was attributed to intermetallic phases (mainly sigma phase) precipitation.

## 1. Introduction

Intergranular corrosion in austenitic stainless steels has been known and investigated for nearly 100 years [1]. A literature search on stainless steels using the key words *intergranular corrosion* or *sensitization* reveals that there are thousands of published works on this subject. Nearly 99% of these publications deal with intergranular corrosion due to chromium depletion at the grain boundaries caused by chromium carbide ($M_{23}C_6$) precipitation [2–8]. On the other hand, when austenitic stainless steels are exposed for long periods in the range from 500 °C to 900 °C, the precipitation of a large number of phases, besides $M_{23}C_6$, might occur, such as $M_6C$ and the sigma, chi and Laves intermetallic phases [9–12]. Among the intermetallic phases that might precipitate in stainless steels, the sigma phase is the best known and studied. The sigma phase is richer in chromium and molybdenum than the austenite phase; therefore its precipitation at the grain boundaries causes the impoverishment of these elements in the adjacent matrix. Despite this, the effect of this precipitation on the stainless steel intergranular corrosion resistance has not been widely investigated [13–16].

The susceptibility to intergranular corrosion is decreased in stainless steels by reducing their carbon content to less than 0.03 wt.%; the main types of this stainless steel class are AISI 304L and 316L. Nevertheless, the decrease in carbon content reduces still further the low yield strength of the austenite in these steels in the annealed condition. Nitrogen might be

---

[*] *Corresponding author.*
*E-mail addresses:* maysaterada@uol.com.br (M. Terada), padilha@usp.br (A.F. Padilha).

1044-5803/$ – see front matter © 2007 Elsevier Inc. All rights reserved.
doi:10.1016/j.matchar.2007.05.017

**Table 1 – Chemical composition of the AISI 316L(N) austenitic stainless steel (wt.%)**

| C | Si | Mn | P | S | Cr | Ni | Mo | Cu | N | Al | B | Fe |
|---|---|---|---|---|---|---|---|---|---|---|---|---|
| 0.02 | 0.32 | 1.80 | 0.02 | 0.006 | 17.34 | 12.50 | 2.40 | 0.12 | 0.08 | 0.018 | 0.0014 | Balance |

added in order to counteract this effect, as is the case with AISI 316L(N). Nitrogen in solid solution in the austenite phase increases the strength, stabilizes the austenite and increases the pitting resistance [17–20].

The effect of very long periods of aging on the corrosion resistance of stainless steels has not been widely studied owing mainly to the difficulties and costs associated with long-duration aging treatments.

In this study, the effects of precipitation, mainly of sigma phase, on the corrosion resistance of AISI 316L(N) stainless steel previously exposed in creep tests at 600 °C [20,21] for periods of up to 10 years, have been investigated.

## 2. Experimental Procedure

The material used in this study was a AISI 316L(N) stainless steel (SS) whose chemical composition is shown in Table 1. AISI 316L(N) SS samples were solution-annealed at 1100 °C for 30 min and then water-quenched, resulting in samples with average grain size of 120 μm. Residual δ-ferrite stringers were detected after solution annealing and before creep testing [20]. The specimens for creep tests were taken from the center of the solution-annealed plate, in the transverse-to-rolling direction. During the creep test, the temperature was maintained at 600 °C and it was continuously measured with a thermocouple. Table 2 shows the conditions used for the creep test (stress, time). Two distinct specimens, identified as *H* and *G*, were tested for periods of 7500 h and 85,000 h, respectively.

For corrosion resistance evaluation, the surface of the AISI 316L(N) SS was prepared by grinding with SiC paper #600. The specimens were then immersed in a test solution composed of 2 M $H_2SO_4$+0.5 M NaCl+0.01 M KSCN at 30 °C, and then, anodic potentiodynamic polarization and double loop electrochemical potentiokinetic reactivation (DL-EPR) tests were carried out. Electrochemical impedance spectroscopy (EIS) tests were also carried out in the electrolyte described above. A three-electrode set-up cell was used, with a saturated calomel electrode (SCE) as the reference electrode, a platinum wire as the counter electrode and the specimen as the working electrode. All potentials in this work are referred to the SCE electrode. EIS measurements were accomplished using a 1255 Solartron frequency response analyser coupled to an EG&G 273A potentiostat. All EIS measurements were obtained in the potentiostatic mode at the open-circuit potential (OCP). The amplitude of the perturbation signal was 10 mV and the frequency range investigated was 100 kHz to 10 mHz with an acquisition rate of 6 points per decade. Potentiodynamic polarization measurements were obtained from the OCP up to 2 V at a scan rate of 1 mV/s. In the DL-EPR tests, the specimens were anodically polarized from the corrosion potential up to 1.5 V (SCE) at a scan rate of 1.67 mV/s. At 1.5 V, the polarization direction was reversed and the test was finished at the initially measured OCP. The surfaces exposed to the electrolytes were observed by scanning electron microscopy (SEM) after the polarization tests using a Philips XL30 microscope.

## 3. Results and Discussion

Fig. 1 shows the EIS results for AISI 316L(N) SS in 2 M $H_2SO_4$+ 0.5 M NaCl+0.01 M KSCN solution, as Bode phase angle (a) and Nyquist (b) diagrams. Solution-annealed samples and samples solution-annealed and aged during creep testing (600 °C/7500 h and 600 °C/85,000 h) were evaluated.

The Bode phase angle diagrams show only a phase angle peak at frequencies around $10^2$ Hz suggesting only a single time constant, likely due to charge transfer processes at the stainless steel-solution interface. The similarity of the diagrams obtained for the three tested conditions also suggests that the corrosion mechanism is analogous for all the samples. The highest phase angle peaks were associated with solution-annealed samples. The phase angle peak decreased and moved to higher frequencies with aging time indicating that the charge transfer process kinetics was favored in the aged samples. The Nyquist diagrams (Fig. 1B) show a well defined capacitative loop with low frequency impedance limit that decreases from the solution-annealed samples to the samples creep tested for 85,000 h. The significant impedance decrease with creep testing time (around one order of magnitude) indicates increasingly faster charge transfer processes at the surface of the creep tested samples.

The EIS results were supported by the potentiodynamic polarization curves, as Fig. 2 shows. All samples showed an active–passive transition; however the current densities in the passive range were much lower for the solution-annealed samples (order of $10^{-6}$ A cm$^{-2}$), indicating the formation of a more protective film on the solution-annealed samples than on those that were creep tested. In fact, the current densities at the corrosion potential associated with these last types of samples were on the order of $10^{-4}$ A cm$^{-2}$, suggesting that the surface film formed on these samples is not very protective and partial dissolution of metallic material occurs through this film. The large amounts of precipitates in the creep tested

**Table 2 – Conditions of creep tests at 600 °C of AISI 316L(N) specimens [21]**

| Sample | Stress (MPa) | Time (h) | Initial strain (%) | Specimens dimension; diameter × length (mm) |
|---|---|---|---|---|
| H | 170 | 7500 | 5.0 | 8×200 |
| G | 70 | 85,000 | 0.005 | 8×200 |

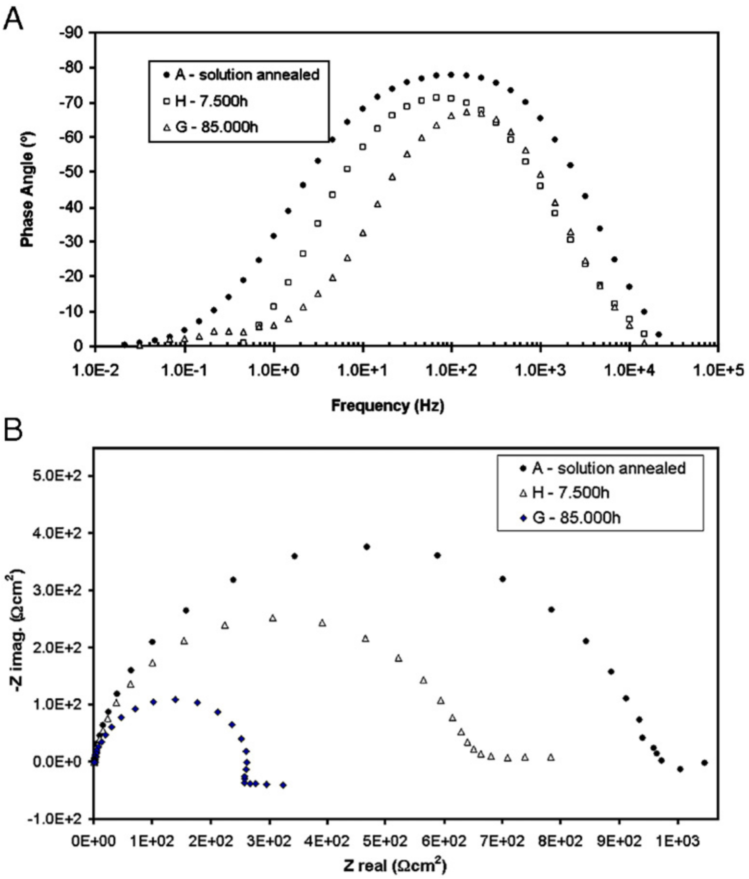

**Fig. 1 – EIS results as (A) Bode phase angle and (B) Nyquist diagrams obtained in 2 M $H_2SO_4$ + 0.5 M NaCl + 0.01 M KSCN solution for AISI 316L(N) SS solution-annealed (*A*) and solution-annealed and creep tested at 600 °C for 7500 h (*H*) and 85,000 h (*G*).**

samples impair the formation of a continuous and protective oxide film on their surfaces.

Despite the slightly lower tendency to passivation observed for the creep tested samples during 85,000 h compared to 7500 h, as indicated by the lower $i_{max}$ previous to passivation, the polarization curves did not allow a clear distinction between the electrochemical behavior of the samples creep tested for these different times. This could be due to the highly aggressive nature of the test solution used, which is usually adopted for intergranular corrosion susceptibility evaluation. The results also show that the solution-annealed samples did not show a large potential range of passive stability. In fact, the current density starts increasing after it has reached a minimum at potentials around 0.4 V. This could be related to the initiation of localized corrosion processes on the solution-annealed samples.

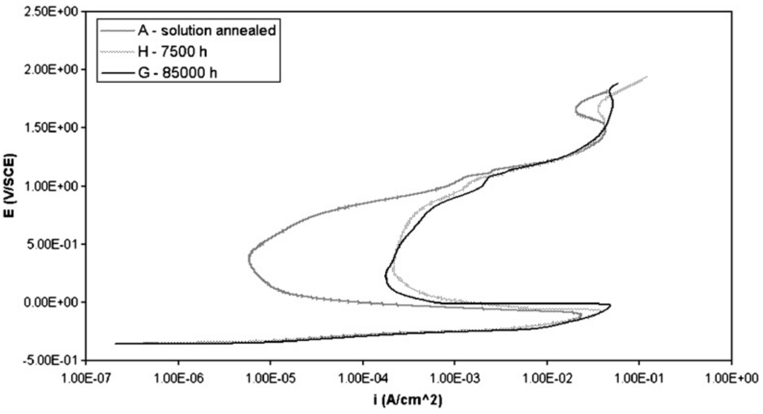

**Fig. 2 – Potentiodynamic polarization curves for solution-annealed and solution-annealed and creep tested AISI 316 L(N) samples tested for 7500 h and 85,000 h at 600 °C, in 2 M $H_2SO_4$ + 0.5 M NaCl + 0.01 M KSCN solution.**

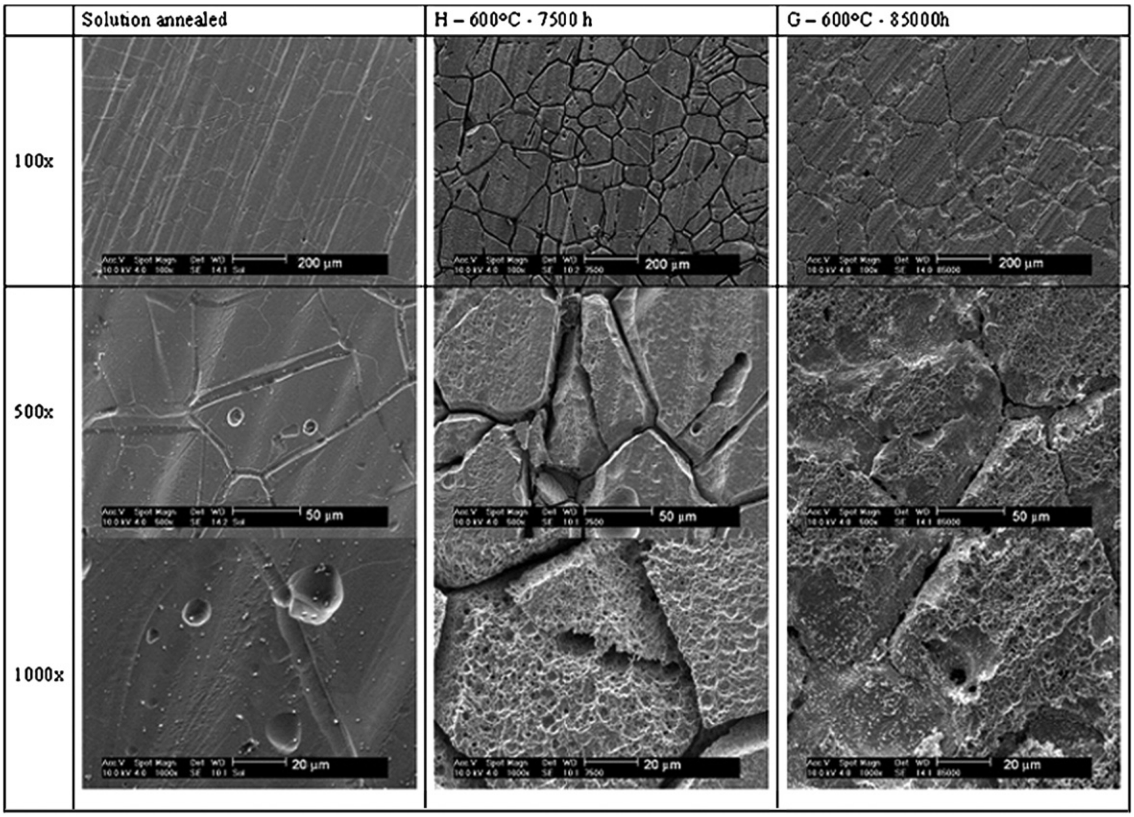

**Fig. 3 – SEM micrographs after potentiodynamic polarization tests for the AISI 316 L(N) solution-annealed and solution-annealed and creep tested for 7500 h and 85,000 h at 600 °C.**

Micrographs of the samples after the polarization tests are shown in Fig. 3. These micrographs indicate a slight attack at the grain boundaries and at the twin boundaries of the solution-annealed sample, but for the samples creep tested during 7500 h the grain boundary regions are intensely attacked. At higher magnifications, there is also evidence of intense corrosion inside the grains of these specimens. Severe attack of the samples creep tested for 85,000 h, either inside the grains or at the grain boundaries, resulted in large material loss from these areas. Consequently, the attack at the grain boundaries for these samples was apparently shallower than for those creep tested during 7500 h, as it is clearly seen at lower magnifications (Fig. 3). A potential contributor to the apparently more aggressive grain boundary attack in the 7500 h creep sample was the much higher chromium gradient for this specimen compared to that used for the 85,000 h specimen. It is proposed that the corrosive attack inside the grains nucleated at microgalvanic cells, between the matrix and

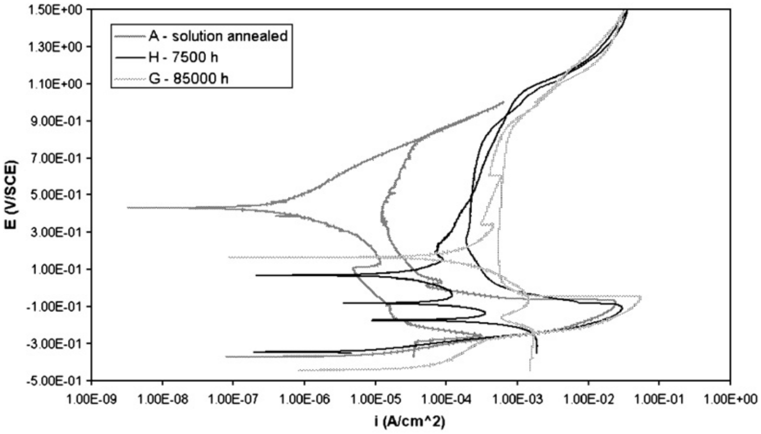

**Fig. 4 – DL-EPR results for AISI 316 L(N) solution-annealed and solution-annealed and creep tested for 7500 h and 85,000 h at 600 °C.**

small precipitates, easily seen in Fig. 3 at lower magnifications, leading to localized corrosion, as pits. The large number of these pits inside the grains resulted in a surface morphology typical of generalized attack, as can be seen at higher magnifications. After the polarization tests, pits were more easily identified on the solution-annealed samples, most likely due to the passive regions surrounding them [14,22].

These results might be explained by the microstructure of the SS samples [2,7,16,19,22]. Copious sigma phase precipitation occurred in the creep tested samples, mainly at the grain boundaries and at triple points, leading to preferential attack at these areas. Intragranular precipitation in samples creep tested for long periods might have been the cause of the corrosive attack at these areas. Amirthalingam et al. [16] confirm that after 1000 h of aging it is possible to find a large amount of intragranular sigma phase in this type of sample.

The precipitation behavior of this heat of AISI 316L(N) was studied previously during long-term creep tests at 550 and 600 °C [20]. Three phases were detected: $M_{23}C_6$, sigma, and Laves phases. The volume fraction of the precipitated sigma phase was significantly higher than those of the carbides and the Laves phase. Precipitation during creep testing commenced with the rapid formation of $M_{23}C_6$ at grain boundaries of the initially solution-annealed specimens. Carbide precipitation was followed by sigma phase formation in the delta ferrite islands via the eutectoid reaction $\delta \rightarrow \sigma + \gamma$. The sigma phase precipitated at grain boundaries after longer times. The Laves phase precipitated concurrently with the sigma phase in delta ferrite and at grain boundaries. After longer exposure times, it also precipitated intragranularly. After long-term exposures, grain boundary carbides were not found [20]. Intermetallic phase precipitation results in a depletion of chromium and molybdenum in the adjacent matrix. It is known that the carbon solubility in austenite increases significantly with decreasing molybdenum and chromium content, resulting in the resolution of precipitated $M_{23}C_6$ carbides [9].

In order to quantitatively evaluate the intergranular corrosion resistance of the 316 L(N) at the various conditions tested, the double loop electrochemical potentiokinetic reactivation technique (DL-EPR) was used. This method is based on passivation followed by reactivation of the stainless steel surface from the passive state. Fig. 4 shows representative polarization curves obtained by the DL-EPR method for the three types of samples tested. The maximum anodic current ($i_a$) is obtained from the polarization curve corresponding to the scan in the anodic direction. At 1.5 V, the polarization direction was reversed, and when reactivation of the surface occurs the maximum current obtained during the reverse scan corresponds to the reactivation current ($i_r$). For sensitized steels, reactivation occurs preferentially at the grain boundaries and the ratio ($i_r/i_a$) indicates the susceptibility to intergranular corrosion.

Table 3 – Values of ($i_r/i_a$) obtained from the DL-EPR for AISI 316 L(N)

| Heat treatment | $i_r/i_a$ |
|---|---|
| A — solution-annealed | 0.00024 |
| H — solution-annealed + 7500 h at 600 °C | 0.00045 |
| G — solution-annealed + 85,000 h at 600 °C | 0.0110 |

Table 3 presents a summary of the $i_r/i_a$ values obtained from the DL-EPR method for the various conditions tested. The results show that the aging treatment at 600 °C for 7500 h reduced the intergranular corrosion resistance of the steel by a factor of approximately two, whereas for samples aged for 85,000 h, the intergranular corrosion resistance decreased by more than a factor of 45.

The DL-EPR tests confirmed the other electrochemical results showing that the susceptibility to intergranular corrosion increases with creep testing time [3,20].

## 4. Conclusions

The susceptibility to intergranular corrosion of the AISI 316 L (N) was highly affected by aging at 600 °C and creep testing time. The tendency to passivation decreased and less protective films were formed on the samples exposed for long periods at 600 °C. The susceptibility to intergranular corrosion increased by more than a factor of twenty when the creep testing time increased from 7500 h to 85,000 h. All samples tested also showed susceptibility to pitting, but in the samples exposed for 85,000 h the very large number of pit nucleation sites observed suggested a generalized attack on their surfaces. Grain boundary $M_{23}C_6$ carbides were not found after long-term exposure at 600 °C; the corrosion behavior of the creep tested samples may be attributed to the precipitation of intermetallic phases (mainly sigma phase).

## Acknowledgements

The authors acknowledge CAPES and for financial support. One of the authors (AFP) wishes to thank FAPESP (S. Paulo, Brazil) for the granting of a visiting fellowship in Germany.

## REFERENCES

[1] Padilha AF, Plaut RL, Rios PR. Stainless steels heat treatment (Chapter 12). In: Totten GE, editor. Steel Heat Treatment Handbook. Second Edition. Boca Raton (FL, USA): CRC Press; 2007. p. 695–739.

[2] Zingales A, Quartarone G, Moretti G. Sigma phase intergranular corrosion effects in austenitic welds containing ferrite. Corrosion 1985;41:136–41.

[3] Muraleedharan J, Gnanamoorthy B, Rodriguez P. Comparative study: degree of sensitization and intergranular stress corrosion cracking susceptibility of type 304 stainless steel. Corrosion 1996;52:790–800.

[4] Chattoraj I, Bhattamishra AK, Jana S, Das SK, Chakraborty SP, De PK. The association of potentiokinetic reactivation and electrochemical pitting tests on a nitrogen bearing 19Cr-17Mn steel with its thermal history. Corr Sci 1996;38:957–69.

[5] Shankar P, Shaikh H, Sivakumar S, Venugopal S, Sundararaman D, Khatak HS. Effect of thermal aging on the room temperature tensile properties of AISI type 316LN stainless steel. J Nucl Mater 1999;264:29–34.

[6] Sahlaoui H, Makhlouf K, Sidhom H, Philibert J. Effect of ageing conditions on the precipitates evolution, chromium depletion

and intergranular corrosion susceptibility of AISI 316L: experimental and modeling results. Mater Sci Eng A 2004;372:98–108.

[7] Stonawska Z, Svoboda M, Sozanska M, Kristková M, Sojka J, Dagbert C, Hyspecka L. Structural analysis and intergranular corrosion tests of AISI 316L steel. J Microsc 2006;224:62–4.

[8] Terada M, Saiki M, Costa I, Padilha AF. Microstructure and intergranular corrosion of the austenitic stainless steel 1.4970. J Nucl Mater 2006;358:40–6.

[9] Weiss B, Stickler R. Phase instabilities during high temperature exposure of 316 austenitic stainless steel. Metall Trans 1972;3:851–66.

[10] Barcik J. Mechanism of sigma-phase precipitation in Cr–Ni austenitic steels. Mater Sci Technol 1988;4:5–15.

[11] Matula M, Hyspecka L, Svoboda M, Vodarek V, Dagbert C, Galland J, et al. Intergranular corrosion of AISI 316L steel. Mater Charact 2001;46:203–10.

[12] Padilha AF, Rios PR. Decomposition of austenite in austenitic stainless steels. ISIJ Int (Japan) 2002;42:325–37.

[13] Zingales A, Quartarone G, Moretti G. Sigma phase intergranular corrosion effects in austenitic welds containing ferrite. Corrosion 1985;41:136–41.

[14] Ganesan V, Ganesan V. Corrosion of annealed AISI 316 stainless steel in sodium environment. J Nucl Mater 1998;256:69–77.

[15] Lin D-Y, Wu W, Lin CH, Hsieh H-H. The effect of aging on the intergranular corrosion of a 24Cr–14Ni–0.7Si stainless steel welding in architecture. Steel Res 2001;72:277–80.

[16] Amirthalingam R, Shaikh H, Anita T, Poonguzhali A, Manohar P, Khatak HS. Effect of high temperature ageing on the corrosion behaviour of nitrogen-added AISI type 316L stainless steel. T Indian I Metals 2006;59:271–82.

[17] Newman RC, Shahrabi T. The effect of alloyed nitrogen or dissolved nitrate ions on the anodic behavior of austenitic stainless steel in hydrochloric acid. Corr Sci 1987;27:827–38.

[18] Rhodes GO, Conway JJ. High nitrogen austenitic stainless steels with high strength and corrosion resistance. Jom 1996;48:28–31.

[19] Ningshen S, Mudali UK, Amarendra G, Golapan P, Dayal RK, Khatak HS. Hydrogen effects on the passive film formation and pitting susceptibility of nitrogen containing type 316L stainless steels. Corr Sci 2006;48:1106–21.

[20] Padilha AF, Escriba DM, Materna-Morris E, Rieth M, Klimenkov M. Precipitation in AISI 316L(N) during creep tests at 550 and 600 °C up to 10 years. J Nucl Mater 2007;362:132–8.

[21] M. Schirra, A. Falkenstein, S. Heger: Experimentelle Ergebnisse zum Kriechenverhalten des Strukturwerkstoffes 316-L(N)-DIN 1.4909 im niedrigen Spannungsbereich bei 550° und 600 °C (Abschlussbericht), Report FZKA 6699, Karlsruhe Research Center, Germany, February 2002.

[22] Mudali UK, Dayal RK, Gnanamoorthy JB, Rodriguez P. Relationship between pitting and intergranular corrosion of nitrogen-bearing austenitic stainless steels. ISIJ Int 1996;36:799–806.